Supplementing Information

Table S1. Operational characteristics of radiometric sensors.

Features	PAR
Manufacturer	Apogee Instrument
Models	SQ-500-SS
Spectral Range (nm)	389 to 692
Response time (ms)	Less than 1
Directional (cosine) Response	± 5 % at 75° solar zenith angle
Operating Environment	-40 to 70 °C; 0 to 100 % relative humidity; can be submerged in water up to depths of 30 m
Units	mmol/m²

Table S2. Landsat and Sentinel images characteristics and in situ measurements.

Landsat Image ID	Year	Path/Row	In situ Date	Image Date	Days differences
LC08_L1TP_233087_20170306_20200905_02_T1	2017	233/87	1st Mar	6 Mar	±5
LC08_L1TP_232087_20171025_20200902_02_T1		232/87	17 Oct	25 Oct	±8
			19 Oct		±6
LC08_L1TP_233087_20180221_20200902_02_T1	2018	233/87	27 Feb	21 Feb	±6
			28 Feb		±7
LC08_L1TP_232087_20180302_20200902_02_T1		232/87	27 Feb	2 Mar	±3
			28 Feb		±2
LC08_L1TP_233087_20181019_20200830_02_T1		233/87	23 Oct	19 Oct	±4
			24 Oct		±5
LC08_L1TP_233087_20190123_20200830_02_T1	2019	233/87	28 Jan	23 Jan	±5
			29Jan		±6
LC08_L1TP_233087_20190224_20200829_02_T1		233/87	26 Feb	24 Feb	±2
			27 Feb		±3
LC08_L1TP_233087_20191123_20200825_02_T1		233/87	19 Nov	23 Nov	±4
			20 Nov		±3
LC08_L1TP_233087_20191209_20200824_02_T1		233/87	3 Dec	9 Dec	±6
			4 Dec		±5
LC08_L1TP_233087_20200126_20200823_02_T1	2020	233/87	28 Jan	26 Jan	±2
			29 Jan		±3
LC08_L1TP_233087_20200227_20200822_02_T1		233/87	24 Feb	27 Feb	±3
			26 Feb		±1
			27 Feb		±0
LC08_L1TP_233087_20200314_20200822_02_T1		233/87	14 Mar	14 Mar	±0
LC08_L1TP_233087_20201109_20210317_02_T1		233/87	10 Nov	9 Nov	±1
			11 Nov		±2
			12 Nov		±3
LC08_L1TP_232087_20201118_20210315_02_T1		233/87	24 Nov	18 Nov	±6
LC08_L1TP_232087_20201204_20210313_02_T1		233/87	26 Nov	4 Dec	±8

Sentinel Image ID	Year	Title/Subtitle	In situ Date	Image Date	Days differences
S2A_MSIL1C_20170307T142851_N0204_R053_T18HYB_20170307T143353	2017	18/HYB	1st Mar	7 Mar	±6
S2B_MSIL1C_20171021T143739_N0205_R096_T18HYB_20171021T144945		18/HYB	17 Oct	21 Oct	±4
			19 Oct		±2
S2A_MSIL1C_20180223T143751_N0206_R096_T18HYB_20180223T193944	2018	19/HBS	27 Feb	23 Feb	±4
			28 Feb		±5
S2A_MSIL1C_20180302T142851_N0206_R053_T19HBS_20180302T192732		19/HBS	27 Mar	2 Mar	±3
			28 Mar		±2
-		-	23 Oct	-	-
			24 Oct		-
S2A_MSIL1C_20190126T142751_N0207_R053_T18HYB_20190126T174932	2019	18/HYB	28 Jan	26 Jan	±2
S2B_MSIL1C_20190131T142759_N0207_R053_T19HBS_20190131T175239		19/HBS	29 Jan	31 Jan	±2
S2A_MSIL1C_20190225T142751_N0207_R053_T18HYB_20190225T175237		18/HYB	26 Feb	25 Feb	±1
S2A_MSIL1C_20190228T143751_N0207_R096_T18HYB_20190228T180016		18/HYB	27 Feb	28 Feb	±1
S2B_MSIL1C_20191120T143729_N0208_R096_T18HYB_20191120T180001		18/HYB	19 Nov	20 Nov	±1
			20 Nov		±0
S2B_MSIL1C_20191207T142729_N0208_R053_T19HBS_20191207T175009		19/HBS	3 Dec	7 Dec	±4
			4 Dec		±3
S2A_MSIL1C_20200124T143651_N0208_R096_T18HYB_20200124T175925	2020	18/HYB	28 Jan	24 Jan	±4
S2B_MSIL1C_20200129T143659_N0208_R096_T18HYB_20200129T175853		18/HYB	29 Jan	29 Jan	±0
S2A_MSIL1C_20200220T142651_N0209_R053_T19HBS_20200220T175302		19/HBS	24 Feb	20 Feb	±4
S2B_MSIL1C_20200225T142729_N0209_R053_T19HBS_20200225T175306		19/HBS	26 Feb	25 Feb	±1
S2B_MSIL1C_20200228T143729_N0209_R096_T18HYB_20200228T175923		18/HYB	27 Feb	28 Feb	±1
S2A_MSIL1C_20200314T143721_N0209_R096_T18HYB_20200314T180039		18/HYB	14 Mar	14 Mar	±0
S2B_MSIL1C_20201015T143729_N0209_R096_T18HYB_20201015T181134		18/HYB	19 Oct	15 Oct	±4
S2A_MSIL1C_20201020T143731_N0209_R096_T18HYB_20201020T181238		18/HYB	20 Oct	20 Oct	±0
S2A_MSIL1C_20201106T142741_N0209_R053_T19HBS_20201106T181041		19/HBS	10 Nov	6 Nov	±4
S2A_MSIL1C_20201116T142731_N0209_R053_T19HBS_20201116T175834		19/HBS	11 Nov	16 Nov	±5
S2A_MSIL1C_20201119T143731_N0209_R096_T18HYB_20201119T181130		18/HYB	12 Nov	19 Nov	±7
S2A_MSIL1C_20201126T142731_N0209_R053_T19HBS_20201126T180345		19/HBS	24 Nov	26 Nov	±2
S2A_MSIL1C_20201126T142731_N0209_R053_T19HBS_20201126T180345		19/HBS	26 Nov	26 Nov	±0

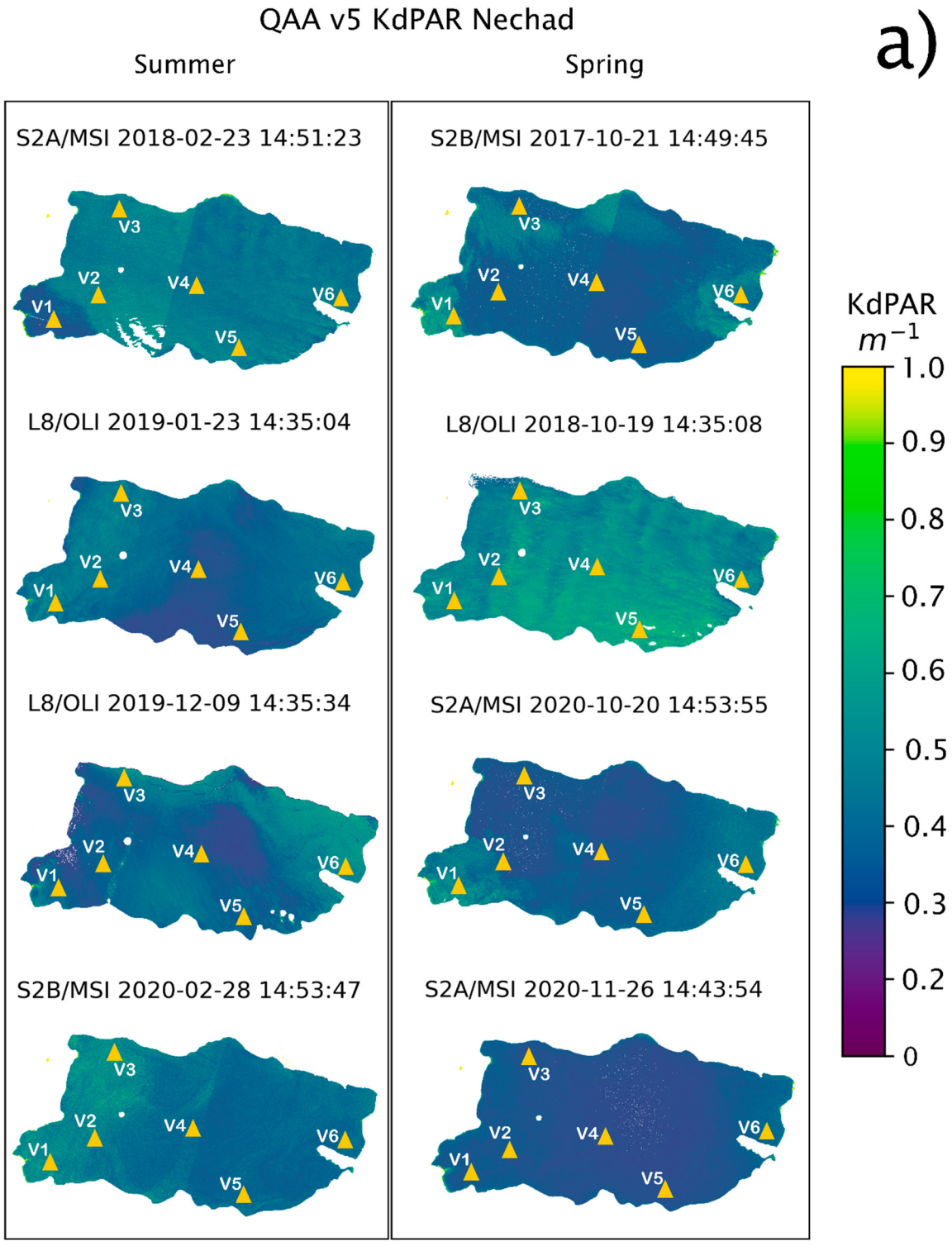
QAA v5 KdPAR Nechad
a)
Summer
Spring
S2A/MSI 2018-02-23 14:51:23
S2B/MSI 2017-10-21 14:49:45
L8/OLI 2019-01-23 14:35:04
L8/OLI 2018-10-19 14:35:08
L8/OLI 2019-12-09 14:35:34
S2A/MSI 2020-10-20 14:53:55
S2B/MSI 2020-02-28 14:53:47
S2A/MSI 2020-11-26 14:43:54
V1
V2
V3
V4
V5
V6
KdPAR
m^{-1}
1.0
0.9
0.8
0.7
0.6
0.5
0.4
0.3
0.2
0

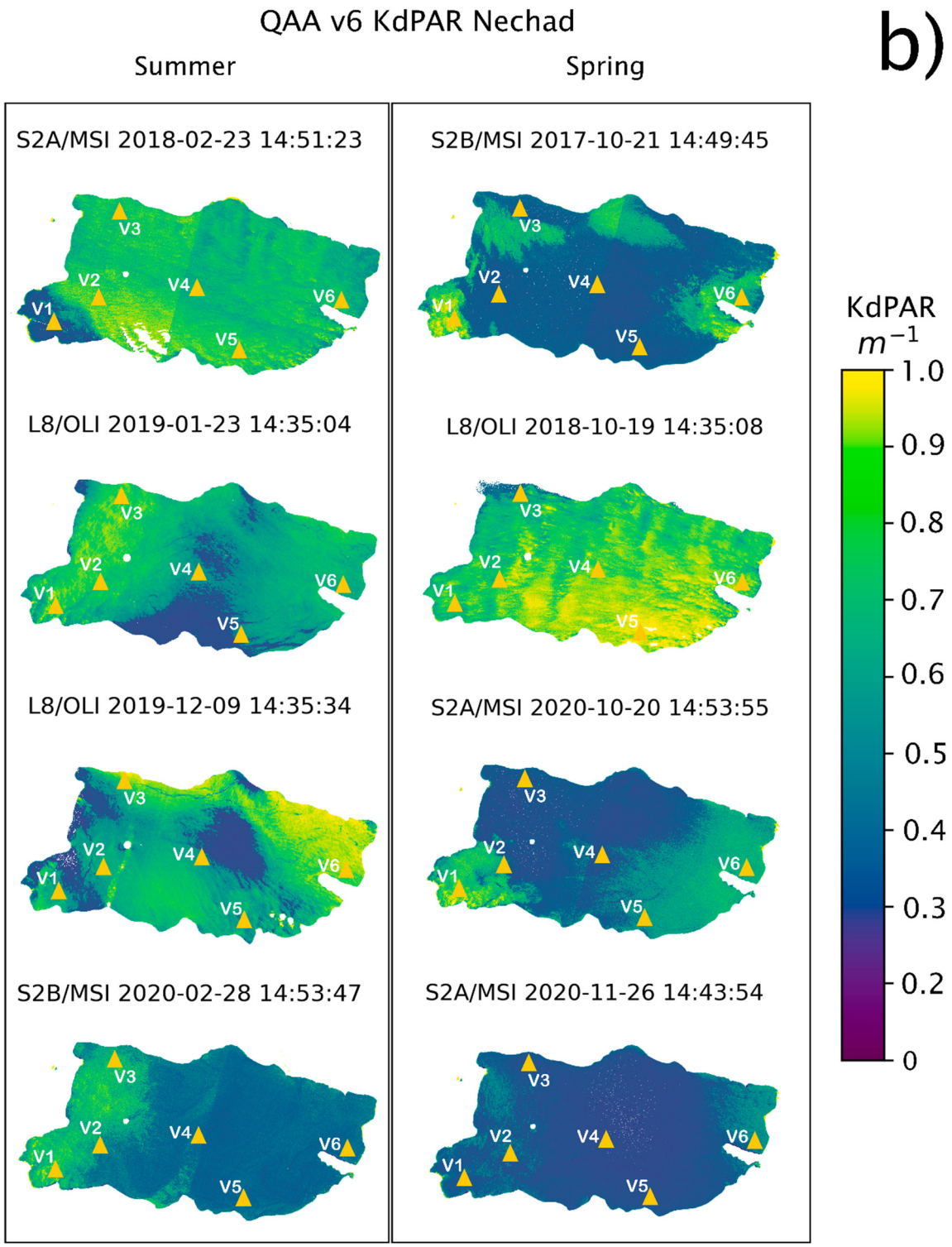
QAA v6 KdPAR Nechad
b)
Summer
Spring
S2A/MSI 2018-02-23 14:51:23
S2B/MSI 2017-10-21 14:49:45
L8/OLI 2019-01-23 14:35:04
L8/OLI 2018-10-19 14:35:08
L8/OLI 2019-12-09 14:35:34
S2A/MSI 2020-10-20 14:53:55
S2B/MSI 2020-02-28 14:53:47
S2A/MSI 2020-11-26 14:43:54
V1
V2
V3
V4
V5
V6
KdPAR
m^{-1}
1.0
0.9
0.8
0.7
0.6
0.5
0.4
0.3
0.2
0

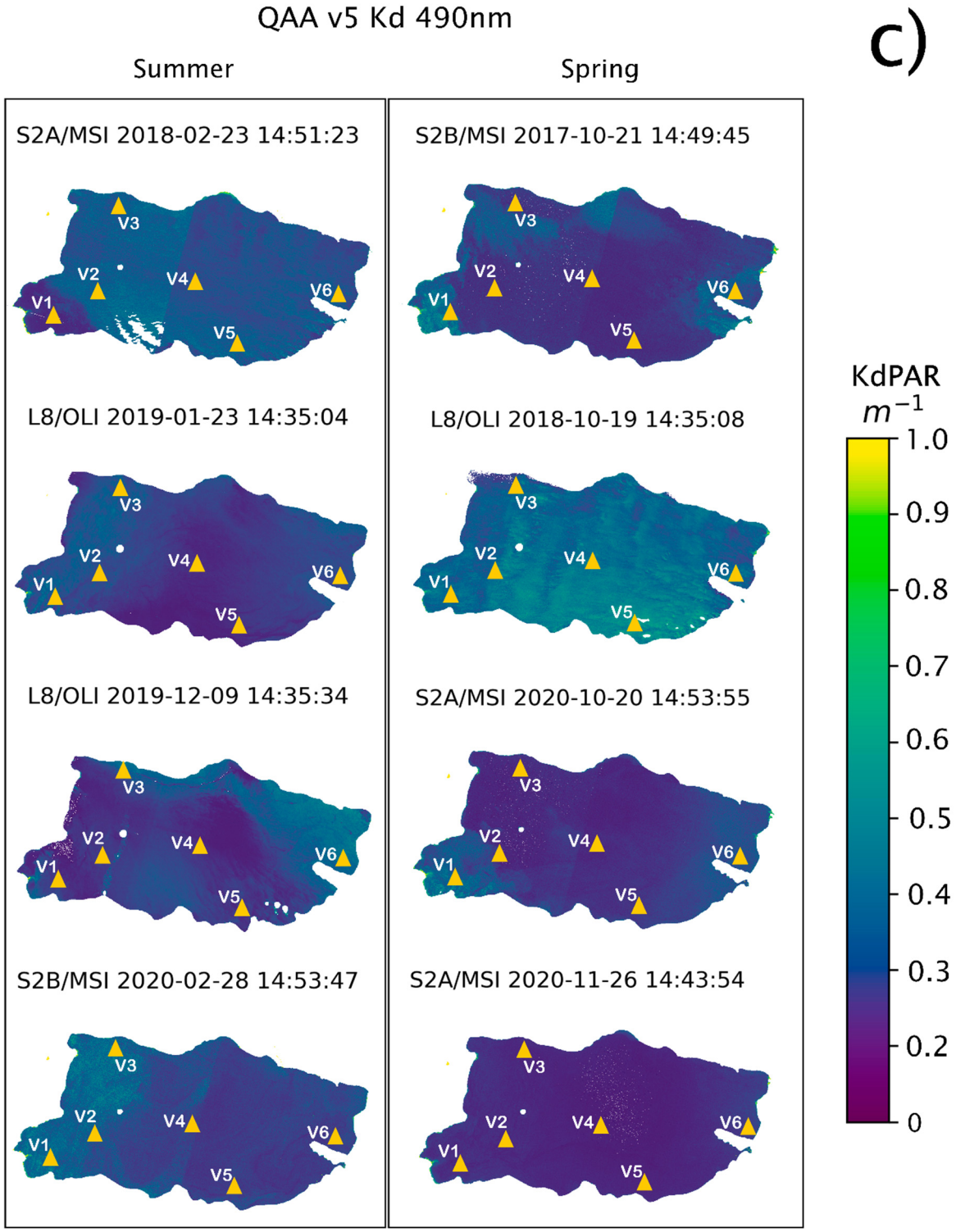
QAA v5 Kd 490nm
c)
Summer
Spring
S2A/MSI 2018-02-23 14:51:23
S2B/MSI 2017-10-21 14:49:45
L8/OLI 2019-01-23 14:35:04
L8/OLI 2018-10-19 14:35:08
L8/OLI 2019-12-09 14:35:34
S2A/MSI 2020-10-20 14:53:55
S2B/MSI 2020-02-28 14:53:47
S2A/MSI 2020-11-26 14:43:54
V1
V2
V3
V4
V5
V6
KdPAR
m^{-1}
1.0
0.9
0.8
0.7
0.6
0.5
0.4
0.3
0.2
0

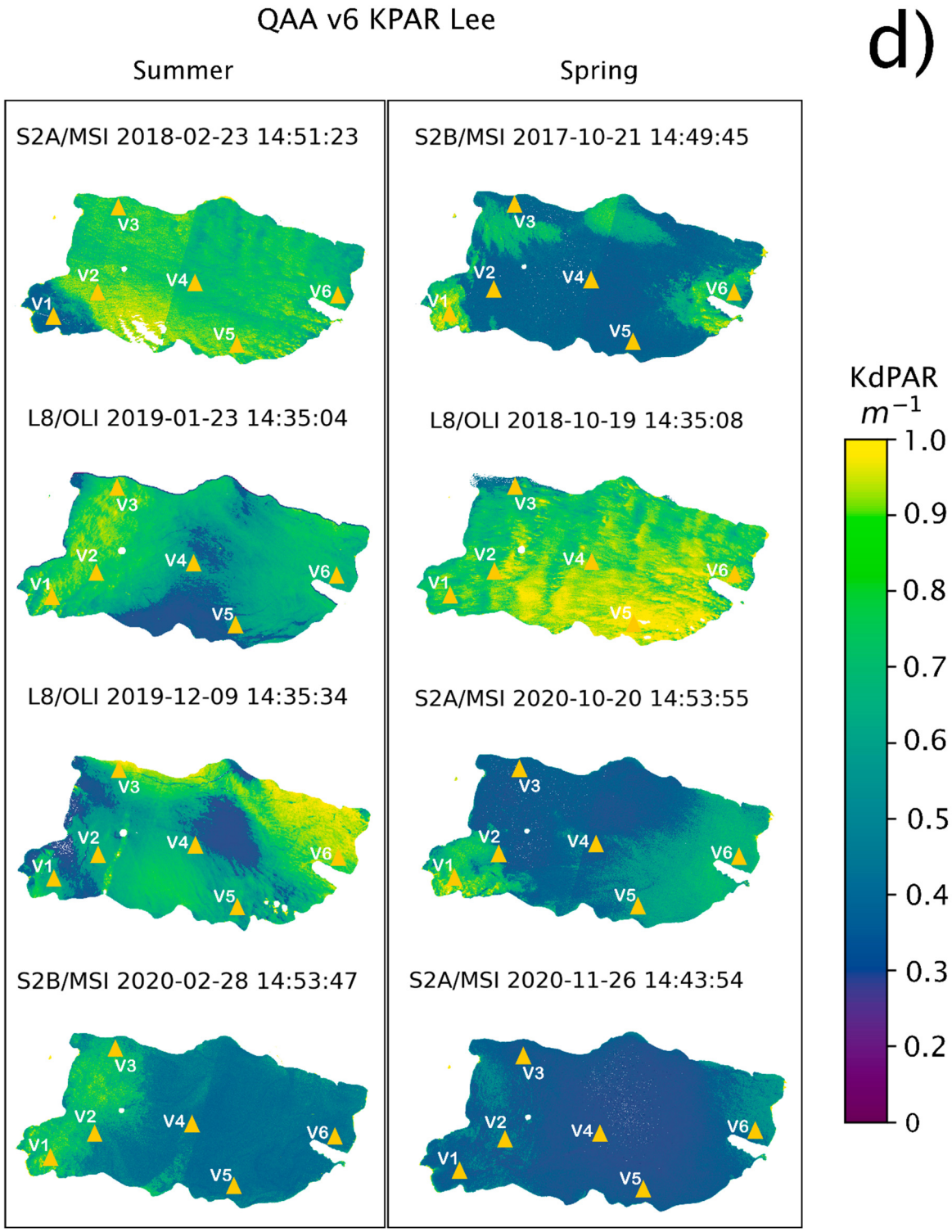

Figure S1. Estimation of KdPAR in the Villarrica lake using the four algorithms runing in L8/OLI and S2A/MSI images. .